Development of new generation fishing gear: A resistant and biodegradable monofilament

Morgan Deroiné [a*], Isabelle Pillin [b], Gwenaël Le Maguer [b], Marie Chauvel [c], Yves Grohens [ab]

[a] *ComposiTIC, Univ. Bretagne Sud, CNRS UMR 6027, IRDL, F-56100 Lorient, France*

[b] *Polymer and Composites, Univ. Bretagne Sud, CNRS UMR 6027, IRDL, F-56100 Lorient, France*

[c] *ICCI Seabird compagny, 7 rue du commandant Charcot, 56260 Larmor-Plage, France*

*Corresponding author: e-mail address: morgan.deroine@univ-ubs.fr
Tel: 02 97 55 08 70

Abstract

Developing biodegradable formulations or controlled-lifetime polymers is one of the issues of tomorrow. In order to reduce the impact of fishing and to fight the expansion of plastic debris in the marine environment, a new generation of monofilament, resistant and biodegradable, has been developed in this study.

The monofilament was obtained by melt-spinning extrusion, and the effect of drawing on the structure and properties of a versatile polymer, poly(butylene succinate) (PBS), was examined. The influence of the draw ratio (3.5, 4, and 4.5) and the drawing oven temperature (60, 80, and 100°C) was investigated, and the modifications obtained by drawing were monitored by means of several characterizations. The mechanical properties of the monofilament before and after drawing were examined by a tensile test. The evolution of the crystallinity and macromolecular chain orientation of the monofilament were determined by thermal analysis (DSC) and Fourier Transform Infra-Red (FTIR) spectroscopy, respectively.

A significant increase in mechanical properties was obtained on a tensile test carried out after drawing. Changes at macromolecular scale were also important: the evolution of crystallinity after drawing was observed and depended on both the temperature and the draw ratio. Then, orientation investigations explained the results obtained through the tensile test and DSC.

The results suggest that poly(butylene succinate) can be an ecofriendly alternative to traditional polyamides commonly used for fishing gear.

Keywords: poly(butylene succinate), PBS, monofilament, fishing line, biodegradable, mechanical properties, orientation

1. Introduction

The first fishing gears were produced using available resources such as cotton, flax, or hemp fibers [1]. Over the last decade, synthetic materials have appeared with the technological development of polyamides (PA) [2,3] and progressively replaced natural fibers. PA became the most commonly used

material for fishing gears, but their environment stability needs to be enhanced against the effects of the weather, such as ultraviolet (UV) degradation [4,5]. The durability of polymers explains their widespread use, but it could also be a considerable drawback in specific cases. Despite the possible fragmentation of polyamides, they remain extremely persistent in the marine environment, and their lifetime is estimated to be over several hundred years [6–8]. Recently, severe environmental pollution by plastic debris has been observed, and their large-scale accumulation in oceanic gyres is now well established [9,10]. In the long term, consequences are devastating for marine wildlife [11,12] with the ghost fishing of macroplastics [13,14], the ingestion of microplastics [15,16], and so on. It is also an uncomfortable reality for fishing activities such as helix blocking or sorting in the nets.

One of the objectives of this study is to develop an ecofriendly monofilament showing high mechanical performance, such as that of the fishing lines currently available. A biopolymer commonly used, poly(butylene succinate) (PBS), appears to be a realistic alternative to conventional materials. PBS is an aliphatic polyester synthetized from petrochemical resources based on 1,4-butandiol and succinic acid, and it is biodegradable. Its properties are comparable to those of traditional polyolefins, and it is mainly used in the packaging field (flexible packaging, coated paper, disposable dishware, etc.) [17].

Biodegradable polymers have already been investigated for marine applications. Some filaments based on polylactide (PLA) exist with the innovative rope Organic® (FSE Robline) or the Elite® BioTwine (LankHorst Yarns). However, PLA is able to biodegrade only under specific conditions [18]. Researchers working with polyhydroxyalkanoates (PHA) have shown that their biodegradation rates are rather fast in marine environments [19–21]. PBS can be degraded in various environments such as soil burial, activated sludge, or compost [22–24], and the biodegradation rate is strongly dependent on its environmental parameters (microorganisms, nutrients, temperature, humidity). The biodegradation of PBS in marine environments, according to a respirometric test such as biochemical oxygen demand (BOD), has already been investigated by Kasuya et al. [25] and shows slow degradation in seawater after one month of immersion at 25°C.

Concerning an application such as fishing gear, the monofilaments used have to be resistant and efficient. In order to enhance the mechanical properties of PBS, some techniques discussed in the literature involve matrix reinforcement with fillers [26] or vegetable fibers [27,28]. Blending PBS with another biopolymer is also used to modulate properties [29,30]. In this study, monofilaments were obtained by melt spinning, and our investigations focused upon the influence of the process parameters on the final properties of the monofilament.

The influence of the draw ratio (3.5, 4, and 4.5) and the drawing oven temperature (60, 80, and 100°C) was examined. The modifications caused by drawing on the mechanical behavior were monitored by tensile tests. The spinning and drawing processes induce severe changes at a molecular scale.

Parameters such as crystallinity and the orientation of the macromolecular chain play an important role in the determination of PBS properties and were also examined. A DSC analysis was performed to monitor thermal properties and the evolution of crystallinity. A polarized Fourier Transform Infra-Red, which is a powerful technique, was used to analyze the orientation [31], as the evaluation of orientation in a polymer provides valuable information for greater understanding of its structure and properties. In the literature, the evolution of crystallinity and orientation has already been examined on PET [32–34], or PS [35,36], but little information is available on PBS. Lyoo *et al*. [37] have worked on the effects of PBS polymer ratio on drawing behavior, but they investigated specific drawing zones on film samples.

In this study, we report the evolution of properties of a potentially useful biodegradable monofilament after drawing and examine the influence of drawing on its thermal and mechanical properties.

2. Experimental setup

2.1 Material

Poly(1,4-butylene succinate) PBS, commercialized in pellet form under the grade BIONOLLE 1001, was supplied by Showa Highpolymer Company (Japan). According to the manufacturer, PBS is a semi-crystalline polymer characterized by a density of 1.25 g.cm^{-1}, a glass transition temperature of -34°C, and a melting temperature of 114°C [38]. PBS pellets were dried at 60°C under vacuum for 12h before processing.

2.2 Preparation of the sample

The monofilaments were prepared by melt-processing using a single-screw extruder with a round nozzle of 2 mm of diameter (Scamex Company - France). The optimal distribution temperatures for PBS spinning were 140-145-145-150°C respectively from the feed zone to the nozzle. The speed of the screw was between 5 and 20 rpm, and the monofilament was cooled via a water bath. After cooling, the monofilament was pulled by a first roll (R1), then went through an oven. Drawing was carried out on line by a second roll (R2). Moreover, drawing a polymer is only possible in a specific temperature range, between the glass transition temperature (T_g) and the melting temperature (T_m). The theoretical drawn ratio (DR_{th}) is expressed as the ratio between the speed of the second roll (V_{R2}) and the speed of the initial roll (V_{R1}) (Eq.1):

$$DR_{th} = \frac{V_{R2}}{V_{R1}} \qquad (Eq.1)$$

The final diameter obtained of undrawn and drawn monofilament is of 1.10 ± 0.05 mm.

2.3 Characterization techniques

2.3.1 Mechanical tests

Tensile tests were performed on an Instron 5566A machine equipped with a 1kN load cell. The monofilaments were tested according to the standard NF EN ISO 2062, under environmentally controlled laboratory conditions (23°C, 50% RH). The main parameters of the test were an initial length of 250 mm, a loading speed of 250 mm.min^{-1} and specific grips for monofilament were used. At least five specimens were tested for each condition, and the results were averaged arithmetically.

Another important parameter in the fishing sector, namely tenacity, was also analyzed. The tenacity of a monofilament is the maximum strength obtained during the tensile test relative to its linear mass (expressed in tex). One of the advantages of this parameter is that the diameter is not taken into account, which enables comparison of all the filaments.

2.3.2 Thermal properties

A differential scanning calorimetry (DSC) analysis was performed on samples of about 10 mg, in standard aluminum pans, using Mettler-Toledo DSC822e equipment under a nitrogen atmosphere. Data were recorded at a heating rate of 20°C.min^{-1}. The samples were heated from 20 to 200°C and kept at 200°C for 2 minutes. The samples were then cooled to -20°C and finally a second heating scan was performed from -20 to 200°C. Thermal transition temperatures were recorded such as the melting temperature (T_m) or the crystallization temperature (T_c) and also the melting enthalpy (ΔH_m) or crystallization enthalpy (ΔH_c), during the first and the second heating. The degree of crystallinity was determined by Eq.2:

$$\chi = \frac{\Delta H_m}{\Delta H_{100\%}} \qquad (Eq.2)$$

where ΔH_m (J.g^{-1} of polymer) is the melting enthalpy obtained during the first heating. $\Delta H_{100\%}$ is the melting enthalpy for PBS of 100% crystallinity, taken to be 200 J.g^{-1} [29].

2.3.3 Polarized Fourier transform infrared (FT-IR)

Static polarized FT-IR spectra were recorded with a minimum of 32 scans per sample at a 4 cm^{-1} spectral resolution using a Bruker Vertex 70 spectrometer equipped with Attenuated Total Reflectance (ATR) module with diamond crystal. All spectra were recorded in the absorbance mode in the 4000-600 cm^{-1} region.

The molecular orientation of a polymer can be quantified by infrared linear dichroism (IRLD) via the dichroic ratio of absorbance between two spectra: one measured with parallel polarized light (A_p) and the other one with a light polarized perpendicularly (A_s) to the direction of stretching. The polarizers were rotated to 0° at 90° and spectrum-recorded, thus enabling a direct measurement of the dichroic ratio:

$$R = \frac{A_p}{A_s} \qquad (Eq.3)$$

Considering uniaxial stretching, the orientation function, <P2>, is related to the dichroic ratio according to the following relationship [39]:

$$\langle P_2 \rangle = \left(\frac{2}{3cos^2\alpha - 1}\right)\left(\frac{R-1}{R+2}\right) \quad (Eq.4)$$

where α is the angle between the transition dipole moment of selected vibration and the main chain axis of the polymer. The limiting values of <P2> are 0 and 1 for random and perfect orientation along the stretching direction, respectively.

3. Results and discussion

3.1 Mechanical properties

Tensile tests were carried out on the undrawn and drawn PBS monofilament. The influence of the oven temperature during drawing was first examined. The mechanical behaviors of the different samples are shown in Figure 1 and the mechanical properties such as Young modulus, stress at break, strain at break, and percentage gain property are summarized in Table 1.

Concerning the undrawn sample, an important ductility is observed. The failure strain exceeds 500% (Table 1) with a low elastic modulus equal to 564 MPa, close to the mechanical properties of traditional polyolefin [40]. After drawing and for all the drawing temperatures, the monofilament behaviors significantly evolve compared to the undrawn PBS (Figure 1a). An initial elastic linear behavior is observed with an important increase in the stress at break from 64 MPa to 267 MPa and a decrease of strain in the break from 500% to 122.7%, for an oven temperature of 80°C and a drawn ratio of 4 in particular (Table 1).

Moreover, for a constant draw ratio of 4, a small influence of the oven temperature is noted up to 80°C, with a slight evolution of strain at break between 60°C and 80°C from 214 MPa to 267 MPa. For a drawing at 100°C, the curve behavior is lower than 80°C and for all mechanical properties, strain at break reaches only 243 MPa. At 100°C, we can assume the drawing temperature is close to the melting temperature of 114°C, with a possible onset of melting on chain mobility. We observe that at 60°C, no melting is present during drawing, and the gain in mechanical properties is similar to that obtained during cold drawing. At the highest used temperature (100°C), we can assume that a tiny part of PBS begins to melt. Therefore, this melt fraction shows strong mobility and could not contribute to the strain. These macromolecular chains cannot crystallize in spherulites, or only in very small spherulites.

The influence of the draw ratio is shown in Figure 1b. For these tests, the oven temperature was kept constant at 80°C. A significant dependence of the draw ratio on mechanical behaviors is observed. When increasing the draw ratio, the stress at break increases while the strain at break decreases, with a progressive evolution of gain property as shown in Table 1. For example, Young's modulus increases

from 1076 to 1312 to 1483 MPa and stress a break decreases from 148 to 122.7 to 107.6 %, respectively for a drawn ratio of 3.5, 4 and 4.5.

Hot drawing during the process induced significant changes with a potential alignment of the chains of PBS along the drawing direction, which could explain the important increase of the mechanical properties. Although chain mobility seems to be facilitated by the oven temperature up to 80°C, the results indicate a higher influence of the draw ratio on the evolution of mechanical properties than the oven temperature. The optimum processing condition is attained by the on-line spinning and drawing of PBS with a draw ratio of 4.5 and an oven temperature of 80°C.

These tests enable reaching 60% of the strain at break of traditional monofilament in polyamide (personal data). As described in the literature [41], a second drawing could help getting close to the mechanical performance of PA, and we obtained promising first results.

However, further analyses could be investigated for greater understanding of the monofilament behavior such as the evolution of crystallinity or orientation after drawing.

3.2 Thermal analysis

During the spinning process, structural changes appear at molecular level with a reorganization of macromolecular chains. Therefore, the influence of the drawing temperature and ratio on the melting characteristics is shown in Figure 2. Table 2 summarizes the influence of drawing on the thermal transition temperature of PBS (T_m and T_c), enthalpies (ΔH_m and ΔH_c) and crystallinity (χ_c), during the first and second heating scans. The evolution of crystallinity after drawing during the first heating was also investigated.

Considering the undrawn behavior, a first exothermic peak followed by an endotherm peak are observed, corresponding to the melting enthalpy. According to the literature, the PBS melting behavior is well-known to be complex [42]. Indeed, PBS has a melting peak between 112 and 116°C according to its molar mass and thermal history, typically 115.8°C in this study. Its melting behavior is particularly interesting since it shows a complex succession of endotherms during melting. In fact, multiple melting peaks were observed for PBS, varying according to the molar mass, crystallization temperature, cooling rate, and so on. The multiple peak is largely discussed in the literature and is generally ascribed to the co-existence of crystal melting of different stability (dual morphology mechanism) and/or to the melting-recrystallization-melting process [43]. Yoo et *al.* used DSC combined with WAXD to show that no crystal change occurs when PBS is crystallized at different temperatures [44]. It has been concluded that the multiple melting behavior of PBS formed thermally is not due to different crystal modification but can be related to a melting recrystallization process.

The influence of the oven temperature during drawing is shown in Figure 2a. The first exothermic peak corresponding to cold crystallization disappears for each sample after drawing, for a constant

draw ratio. This phenomenon can be explained by a change in morphology caused by the drawing. For a drawing temperature fixed at 80°C (Figure 2b), a melting peak appears at 95°C, but it disappears for a drawing temperature fixed at 60°C and 100°C. Wang et *al*. named this peak Tm_2 and demonstrated that it is temperature dependent [42]. Concerning the mean peak called Tm_1, it appears to widen with the increase of the drawing temperature and could correspond to a thickening of crystalline lamellae. According to the enthalpy value in Table 2, during the first heating, a significant increase is observed between the melting enthalpy of the undrawn and the drawn monofilaments. Moreover, the enthalpy behavior of the drawn monofilament shown in Figure 2a seems to be similar regardless of the temperature, which is directly related to the evolution of crystallinity from 16% for the undrawn monofilament to 31.9, 33.6, and 33.1% for the drawing at a different temperature of 60, 80, and 100°C, respectively. During drawing, the influence of the oven temperature on crystallinity is slight, and this trend is in accordance with the mechanical properties obtained in the previous tests. Lyoo et *al*. [37] obtained similar results, as crystallinity remained nearly constant for a constant draw ratio but with a different initial polymer ratio.

Considering the influence of the drawn ratio shown in Figure 2b, enthalpy modifications are more important with a narrow peak for a ratio of 3.5 and a wider peak for a ratio of 4.5. Moreover, the melting enthalpy progressively increases as a function of the drawn ratio, from 33.2 J/g for the undrawn to 51.9, 67.1, and 68.5 J/g, for a drawn ratio of 3.5, 4, and 4.5, respectively. Concerning the degree of crystallinity, the most important gap is obtained between a drawn ratio from 3.5 to 4, with an increase from 26 to 33.6% respectively. For a ratio of 4.5, the crystallization is closed to the one obtained for a drawn ratio of 4, with a value of 34.2%. From a certain rate of drawing, a limit in the crystallinity fraction is reached. A similar behavior has been already observed for another biopolymer such as PLA [45].

Hot drawing induces the chain mobility. The rearrangement of polymer chains promotes the crystallinity ratio and can explain the different mechanical behaviors of the monofilament obtained after drawing, with an important increase of the mechanical properties (Table 2).

Figure 3 shows the relation between the evolution of tenacity and crystallinity as a function of the different parameters under investigation: the temperature of the oven during drawing (Figure 3a) and the draw ratio (Figure 3b). Considering Figure 3a, the tenacity of the monofilaments slightly increases with the drawing temperature and seems to follow the evolution of crystallinity. At 100°C, the tenacity tends to stabilize at about 19 cN/tex and crystallinity around 33%. The variations induced by the oven temperature parameter are slight and do not significantly influence the mean properties of the PBS monofilament up to 80°C. In Figure 3b, the tenacity of the monofilament is more dependent on the drawn ratio. In fact, the tenacity progressively evolves from 12.4 to 18.5 and 23.5 cN/tex, as a function of the draw ratio from 3.5 to 4.5. In the literature, some authors reported similar values of PBS

tenacity, between 22.6 [46] and 26.9 cN/tex [47], for a draw ratio of 3.7 and 5, respectively. The hot-drawing process with a draw ratio of 4.5 induces high properties for a fishing gear application.

3.3 Orientation investigation by IR

During the drawing step, the macromolecular chains orient in the drawing direction. At equilibrium, the macromolecules have an isotropic random coil configuration. Under the effect of hot drawing, they tend to take a privileged orientation. An optimized cooling at the exit of the die will allow the macromolecular chains to remain oriented by minimizing the effects of relaxation. In this study, the orientation induced by hot drawing has been quantified by Infrared linear dichroic (IRLD).

Figure 4 shows the FTIR spectra of PBS before drawing, in the parallel direction. The main characteristic peaks of PBS are presented below. Two distinct peaks in the region 2980-2850 cm^{-1} correspond to deformation vibrations of CH_2 groups. The band in the 1713 cm^{-1} region is attributed to C=O stretching vibrations of the ester group. The peak at 1155 cm^{-1} is assigned to the C-O-C stretching in the ester linkages of PBS.

The CH_2 symmetric stretching band (2850 cm^{-1}) can be used to evaluate the PBS average orientation function. The α angle is defined between the transition moment and the chain axis, and it is reported to be 70° [35,48]. The absorbance values obtained as a function of the polarization are summarized in Table 3, and the results of the orientation function P_2 are presented in Figure 5.
The orientation function of the undrawn monofilament is first analyzed. The important value obtained for the undrawn monofilament, equal to 0.48, indicates an important orientation during the extrusion process. The capillary flow of the polymer in the die facilitates the orientation of polymer chains along the flow direction. After drawing and considering a constant draw ratio (Figure 5a), the orientation function increases significantly between 60°C and 80°C, with an evolution from 0.58 to 0.73 respectively. These results are congruent with the evolution of the crystallinity and the mechanical properties up to 80°C.

After drawing at 100°C, a slight increase is observed with a value of P2 of 0.76. A stabilization tendency at high temperatures is also observed, close to the melting temperature. The increase of strain is related to the evolution of the orientation chain in PBS, but at 100°C, the mechanical properties of the PBS monofilament are lower. This could be due to the orientation of amorphous chains that can crystallize and could increase the cohesion in the material, inducing higher strain. However, at 100°C, a part of PBS is melted during drawing. Therefore, some crystalline parts contributing to high strain could be disordered, despite the crystallization of a small amorphous part. Moreover, this hypothesis is reinforced by the shoulder observed in the melting peak, which suggests the formation of sperulites with different thermal stabilities depending on their size: new sperulites appear from the amorphous

phase or there is an increase of lamellae thickness of the primary sperulites. Globally, the overall orientation P2 can increase whereas the mechanical strain decreases with a small disruption in the orientation crystalline part.

In Figure 5b, for a constant drawing oven temperature fixed at 80°C, the orientation function increases with the draw ratio. A slight increase is observed between 3.5 and 4, but the most important value is obtained for a draw ratio of 4.5 (0.85). Drawing promotes a macromolecular rearrangement with a preferential alignment of the amorphous and the crystalline chains. This results in closer chain segments, which increases the specific cohesion of the polymer by increasing the orientation, the crystallinity, and the intensity of the molecular interactions, and leads to a significant improvement of the mechanical properties up to a specific temperature of drawing.

These results indicate that drawing is the essential factor to obtain a resistant monofilament. A compromise has to be found between the draw ratio and the temperature. For a further analysis of the draw monofilament orientation, the optical birefringence could be a technique worth considering [35].

4. Conclusion

The aim of the study was to propose a new generation of resistant fishing gear, using a biodegradable polymer. Different tests were carried out on poly(butylene succinate) monofilament. This study shows that PBS is a potentially suitable polymer with versatile properties. The mechanical properties of PBS are known to be closer to traditional polyolefin (PE,PP), but after drawing, significant improvements were observed.

Both parameters under investigation, namely the draw ratio and the temperature of the oven during drawing, are important to enable optimization of the monofilament properties. A high temperature brings chain mobility, and the drawing carried out on line induces a preferential alignment of the macromolecular chains and promotes significant evolution of PBS properties. The higher properties, such as crystallinity, tenacity, and the orientation function, are obtained with a draw ratio of 4.5 and a temperature of 80°C. This draw ratio induced a closer rearrangement of the chain segments, which increases the specific cohesion of the polymer by increasing the crystallinity. Mechanical properties are clearly promoted after drawing and get close to those of polyamides.

This study is a first step in the future development of a biodegradable monofilament. Poly(butylene succinate) could become an eco-friendly alternative to polyamide, particularly used in fishing lines or nets. Moreover, PBS could also be derived from renewable resources with the development of biobased succinic acid [49,50] and 1,4-butandiol [51], but more studies still need to be carried out due to the significant number of secondary products.

The mechanical properties could be increased via a post-drawing step or multi-stage drawing [41]. For a fishing gear application, resistance to abrasion and resistance to knots are two non-negligible criteria

that could be examined. Ageing studies in marine environment (hydrolytic, UV, etc.) are in progress and would help understand the degradation and biodegradation behaviors and predict the lifetime of the monofilament [21]. Finally, as some researchers have indicated the sensitivity of PBS to ultraviolet radiation [52], adjustments could be necessary to optimize the formulation.

Acknowledgements

The authors are grateful to the Bretagne Region for providing financial support for this study.

References

[1] D. Sahrhage, J. Lundbeck, A History of Fishing, Springer Science & Business Media, 2012.
[2] B. Meenakumari, K. Radhalakshmi, P.A. Panicker, Netting materials for low energy fishing gear, Low Energy Fish. Fish Technol Spec. Issue Low Energy Fish. Soc. Fish. Technol. India Cochin. (1993) 107–111.
[3] D.-O. Cho, Removing derelict fishing gear from the deep seabed of the East Sea, Mar. Policy. 35 (2011) 610–614.
[4] R. Shamey, K. Sinha, A review of degradation of nylon 6. 6 as a result of exposure to environmental conditions, Rev. Prog. Color. Relat. Top. 33 (2003) 93–107. doi:10.1111/j.1478-4408.2003.tb00147.x.
[5] S.N. Thomas, C. Hridayanathan, The effect of natural sunlight on the strength of polyamide 6 multifilament and monofilament fishing net materials, Fish. Res. 81 (2006) 326–330. doi:10.1016/j.fishres.2006.06.012.
[6] R.C. Thompson, Y. Olsen, R.P. Mitchell, A. Davis, S.J. Rowland, A.W.G. John, D. McGonigle, A.E. Russell, Lost at Sea: Where Is All the Plastic?, Science. 304 (2004) 838–838. doi:10.1126/science.1094559.
[7] C. Eriksson, H. Burton, Origins and Biological Accumulation of Small Plastic Particles in Fur Seals from Macquarie Island, Httpdxdoiorg1015790044-7447-326380. (2009). http://www.bioone.org/doi/abs/10.1579/0044-7447-32.6.380 (accessed May 23, 2016).
[8] J.A. Ivar do Sul, M.F. Costa, The present and future of microplastic pollution in the marine environment, Environ. Pollut. 185 (2014) 352–364. doi:10.1016/j.envpol.2013.10.036.
[9] J.G.. Derraik, The pollution of the marine environment by plastic debris: a review, Mar. Pollut. Bull. 44 (2002) 842–852. doi:10.1016/S0025-326X(02)00220-5.
[10] C.J. Moore, S.L. Moore, M.K. Leecaster, S.B. Weisberg, A Comparison of Plastic and Plankton in the North Pacific Central Gyre, Mar. Pollut. Bull. 42 (2001) 1297–1300. doi:10.1016/S0025-326X(01)00114-X.
[11] D.K.A. Barnes, A. Walters, L. Gonçalves, Macroplastics at sea around Antarctica, Mar. Environ. Res. 70 (2010) 250–252. doi:10.1016/j.marenvres.2010.05.006.
[12] S. Avery-Gomm, P.D. O'Hara, L. Kleine, V. Bowes, L.K. Wilson, K.L. Barry, Northern fulmars as biological monitors of trends of plastic pollution in the eastern North Pacific, Mar. Pollut. Bull. 64 (2012) 1776–1781. doi:10.1016/j.marpolbul.2012.04.017.
[13] A. Ayaz, D. Acarli, U. Altinagac, U. Ozekinci, A. Kara, O. Ozen, Ghost fishing by monofilament and multifilament gillnets in Izmir Bay, Turkey, Fish. Res. 79 (2006) 267–271. doi:10.1016/j.fishres.2006.03.029.
[14] F. Baeta, M.J. Costa, H. Cabral, Trammel nets' ghost fishing off the Portuguese central coast, Fish. Res. 98 (2009) 33–39. doi:10.1016/j.fishres.2009.03.009.
[15] C.M. Boerger, G.L. Lattin, S.L. Moore, C.J. Moore, Plastic ingestion by planktivorous fishes in the North Pacific Central Gyre, Mar. Pollut. Bull. 60 (2010) 2275–2278. doi:10.1016/j.marpolbul.2010.08.007.

[16] A.L. Bond, J.F. Provencher, P.-Y. Daoust, Z.N. Lucas, Plastic ingestion by fulmars and shearwaters at Sable Island, Nova Scotia, Canada, Mar. Pollut. Bull. 87 (2014) 68–75. doi:10.1016/j.marpolbul.2014.08.010.
[17] J. Xu, B.-H. Guo, Microbial Succinic Acid, Its Polymer Poly(butylene succinate), and Applications, in: Plast. Bact., Springer, Berlin, Heidelberg, 2010: pp. 347–388. doi:10.1007/978-3-642-03287-5_14.
[18] M. Itävaara, S. Karjomaa, J.-F. Selin, Biodegradation of polylactide in aerobic and anaerobic thermophilic conditions, Chemosphere. 46 (2002) 879–885. doi:10.1016/S0045-6535(01)00163-1.
[19] T. Ohura, Y. Aoyagi, K. Takagi, Y. Yoshida, K. Kasuya, Y. Doi, Biodegradation of poly(3-hydroxyalkanoic acids) fibers and isolation of poly(3-hydroxybutyric acid)-degrading microorganisms under aquatic environments, Polym. Degrad. Stab. 63 (1999) 23–29. doi:10.1016/S0141-3910(98)00057-3.
[20] T.G. Volova, A.N. Boyandin, A.D. Vasiliev, V.A. Karpov, S.V. Prudnikova, O.V. Mishukova, U.A. Boyarskikh, M.L. Filipenko, V.P. Rudnev, B. Bá Xuân, V. Việt Dũng, I.I. Gitelson, Biodegradation of polyhydroxyalkanoates (PHAs) in tropical coastal waters and identification of PHA-degrading bacteria, Polym. Degrad. Stab. 95 (2010) 2350–2359. doi:10.1016/j.polymdegradstab.2010.08.023.
[21] M. Deroiné, G. César, A. Duigou, P. Davies, S. Bruzaud, Natural Degradation and Biodegradation of Poly(3-Hydroxybutyrate-co-3-Hydroxyvalerate) in Liquid and Solid Marine Environments, J. Polym. Environ. 4 (2015) 493–505. doi:10.1007/s10924-015-0736-5.
[22] P. Rizzarelli, C. Puglisi, G. Montaudo, Soil burial and enzymatic degradation in solution of aliphatic co-polyesters, Polym. Degrad. Stab. 85 (2004) 855–863. doi:10.1016/j.polymdegradstab.2004.03.022.
[23] J.-H. Zhao, X.-Q. Wang, J. Zeng, G. Yang, F.-H. Shi, Q. Yan, Biodegradation of poly(butylene succinate) in compost, J. Appl. Polym. Sci. 97 (2005) 2273–2278. doi:10.1002/app.22009.
[24] N. Teramoto, K. Urata, K. Ozawa, M. Shibata, Biodegradation of aliphatic polyester composites reinforced by abaca fiber, Polym. Degrad. Stab. 86 (2004) 401–409. doi:10.1016/j.polymdegradstab.2004.04.026.
[25] K. Kasuya, K. Takagi, S. Ishiwatari, Y. Yoshida, Y. Doi, Biodegradabilities of various aliphatic polyesters in natural waters, Polym. Degrad. Stab. 59 (1998) 327–332. doi:10.1016/S0141-3910(97)00155-9.
[26] Y.J. Phua, W.S. Chow, Z.A.M. Ishak, Poly(butylene succinate)/ Organo-montmorillonite Nanocomposites: Effects of the Organoclay Content on Mechanical, Thermal, and Moisture Absorption Properties, J. Thermoplast. Compos. Mater. 24 (2011) 133–151. doi:10.1177/0892705710376469.
[27] L. Liu, J. Yu, L. Cheng, X. Yang, Biodegradability of poly(butylene succinate) (PBS) composite reinforced with jute fibre, Polym. Degrad. Stab. 94 (2009) 90–94. doi:10.1016/j.polymdegradstab.2008.10.013.
[28] T. Yokohara, M. Yamaguchi, Structure and properties for biomass-based polyester blends of PLA and PBS, Eur. Polym. J. 44 (2008) 677–685. doi:10.1016/j.eurpolymj.2008.01.008.
[29] A. Bourmaud, Y.-M. Corre, C. Baley, Fully biodegradable composites: Use of poly-(butylene-succinate) as a matrix and to plasticize l-poly-(lactide)-flax blends, Ind. Crops Prod. 64 (2015) 251–257. doi:10.1016/j.indcrop.2014.09.033.
[30] R. Muthuraj, M. Misra, A.K. Mohanty, Biodegradable Poly(butylene succinate) and Poly(butylene adipate-co-terephthalate) Blends: Reactive Extrusion and Performance Evaluation, J. Polym. Environ. 22 (2014) 336–349. doi:10.1007/s10924-013-0636-5.
[31] I.M. Ward, Structure and Properties of Oriented Polymers, Springer Science & Business Media, 2012.
[32] A. Ajji, J. Guèvremont, K.C. Cole, M.M. Dumoulin, Orientation and structure of drawn poly(ethylene terephthalate), Polymer. 37 (1996) 3707–3714. doi:10.1016/0032-3861(96)00175-9.

[33] K.C. Cole, H. Ben Daly, B. Sanschagrin, K.T. Nguyen, A. Ajji, A new approach to the characterization of molecular orientation in uniaxially and biaxially oriented samples of poly(ethylene terephthalate), Polymer. 40 (1999) 3505–3513. doi:10.1016/S0032-3861(98)00574-6.
[34] A.C. Middleton, R.A. Duckett, I.M. Ward, A. Mahendrasingam, C. Martin, Real-time FTIR and WAXS studies of drawing behavior of poly(ethylene terephthalate) films, J. Appl. Polym. Sci. 79 (2001) 1825–1837. doi:10.1002/1097-4628(20010307)79:10<1825::AID-APP110>3.0.CO;2-S.
[35] B. Jasse, J.L. Koenig, Fourier transform infrared study of uniaxially oriented atactic polystyrene, J. Polym. Sci. Polym. Phys. Ed. 17 (1979) 799–810. doi:10.1002/pol.1979.180170506.
[36] R. Neuert, H. Springer, G. Hinrichsen, Orientation analysis of uniaxially drawn polystyrene films doped with fluorescent molecules by fluorescence polarization, UV-and IR-dichroism and birefringence, Colloid Polym. Sci. 263 (1985) 392–395. doi:10.1007/BF01410386.
[37] W.S. Lyoo, J.H. Kim, W.S. Yoon, B.C. Ji, J.H. Choi, J. Cho, J. Lee, S.B. Yang, Y. Yoo, Effects of polymer concentration and zone drawing on the structure and properties of biodegradable poly(butylene succinate) film, Polymer. 41 (2000) 9055–9062. doi:10.1016/S0032-3861(00)00154-3.
[38] T. Fujimaki, Processability and properties of aliphatic polyesters, 'BIONOLLE', synthesized by polycondensation reaction, Polym. Degrad. Stab. 59 (1998) 209–214. doi:10.1016/S0141-3910(97)00220-6.
[39] T. Buffeteau, B. Desbat, M. Pezolet, J.M. Turlet, ORIENTATIONAL STUDIES OF POLYMERS USING POLARIZATION MODULATION INFRARED LINEAR DICHROISM - EXPERIMENTAL PROCEDURE AND QUANTITATIVE-ANALYSIS, J. Chim. Phys. Phys.-Chim. Biol. 90 (1993) 1467–1489.
[40] E. Frollini, N. Bartolucci, L. Sisti, A. Celli, Poly(butylene succinate) reinforced with different lignocellulosic fibers, Ind. Crops Prod. 45 (2013) 160–169. doi:10.1016/j.indcrop.2012.12.013.
[41] I.-C. Wang, M.G. Dobb, J.G. Tomka, Polypropylene Fibres: An Industrially Feasible Pathway to High Tenacity, J. Text. Inst. 86 (1995) 383–392. doi:10.1080/00405009508658765.
[42] X. Wang, J. Zhou, L. Li, Multiple melting behavior of poly(butylene succinate), Eur. Polym. J. 43 (2007) 3163–3170. doi:10.1016/j.eurpolymj.2007.05.013.
[43] G.Z. Papageorgiou, D.N. Bikiaris, Crystallization and melting behavior of three biodegradable poly(alkylene succinates). A comparative study, Polymer. 46 (2005) 12081–12092. doi:10.1016/j.polymer.2005.10.073.
[44] E.S. Yoo, S.S. Im, Melting behavior of poly(butylene succinate) during heating scan by DSC, J. Polym. Sci. Part B Polym. Phys. 37 (1999) 1357–1366. doi:10.1002/(SICI)1099-0488(19990701)37:13<1357::AID-POLB2>3.0.CO;2-Q.
[45] B. Gupta, N. Revagade, J. Hilborn, Poly(lactic acid) fiber: An overview, Prog. Polym. Sci. 32 (2007) 455–482. doi:10.1016/j.progpolymsci.2007.01.005.
[46] K. Twarowska-Schmidt, W. Tomaszewski, Evaluation of the Suitability of Selected Aliphatic Polyester Blends for Biodegradable Fibrous Materials with Improved Elasticity, Fibres Text. East. Eur. 68 (2008). http://www.fibtex.lodz.pl/article159.html (accessed November 6, 2017).
[47] S. Nakano, A.E. Salmawy, T. Nakamura, Y. Kimura, Properties and Enzymatic Degradability of Melt-Spun Fibers of Poly(butylene succinate) and Its Various Dertivatives, 繊維学会誌. 58 (2002) 209–215. doi:10.2115/fiber.58.209.
[48] M.A. Fourati, C. Pellerin, C.G. Bazuin, R.E. Prud'homme, Infrared and fluorescence spectroscopy investigation of the orientation of two fluorophores in stretched polymer films, Polymer. 54 (2013) 730–736. doi:10.1016/j.polymer.2012.11.063.
[49] I. Bechthold, K. Bretz, S. Kabasci, R. Kopitzky, A. Springer, Succinic Acid: A New Platform Chemical for Biobased Polymers from Renewable Resources, Chem. Eng. Technol. 31 (2008) 647–654. doi:10.1002/ceat.200800063.
[50] J. Xu, B.-H. Guo, Poly(butylene succinate) and its copolymers: Research, development and industrialization, Biotechnol. J. 5 (2010) 1149–1163. doi:10.1002/biot.201000136.
[51] H. Yim, R. Haselbeck, W. Niu, C. Pujol-Baxley, A. Burgard, J. Boldt, J. Khandurina, J.D. Trawick, R.E. Osterhout, R. Stephen, J. Estadilla, S. Teisan, H.B. Schreyer, S. Andrae, T.H. Yang, S.Y. Lee,

M.J. Burk, S. Van Dien, Metabolic engineering of Escherichia coli for direct production of 1,4-butanediol, Nat. Chem. Biol. 7 (2011) 445–452. doi:10.1038/nchembio.580.

[52] M.Z.A. Thirmizir, Z.A.M. Ishak, R.M. Taib, R. Sudin, Y.W. Leong, Mechanical, Water Absorption and Dimensional Stability Studies of Kenaf Bast Fibre-Filled Poly(butylene succinate) Composites, Polym.-Plast. Technol. Eng. 50 (2011) 339–348. doi:10.1080/03602559.2010.531871.

Figures and Tables

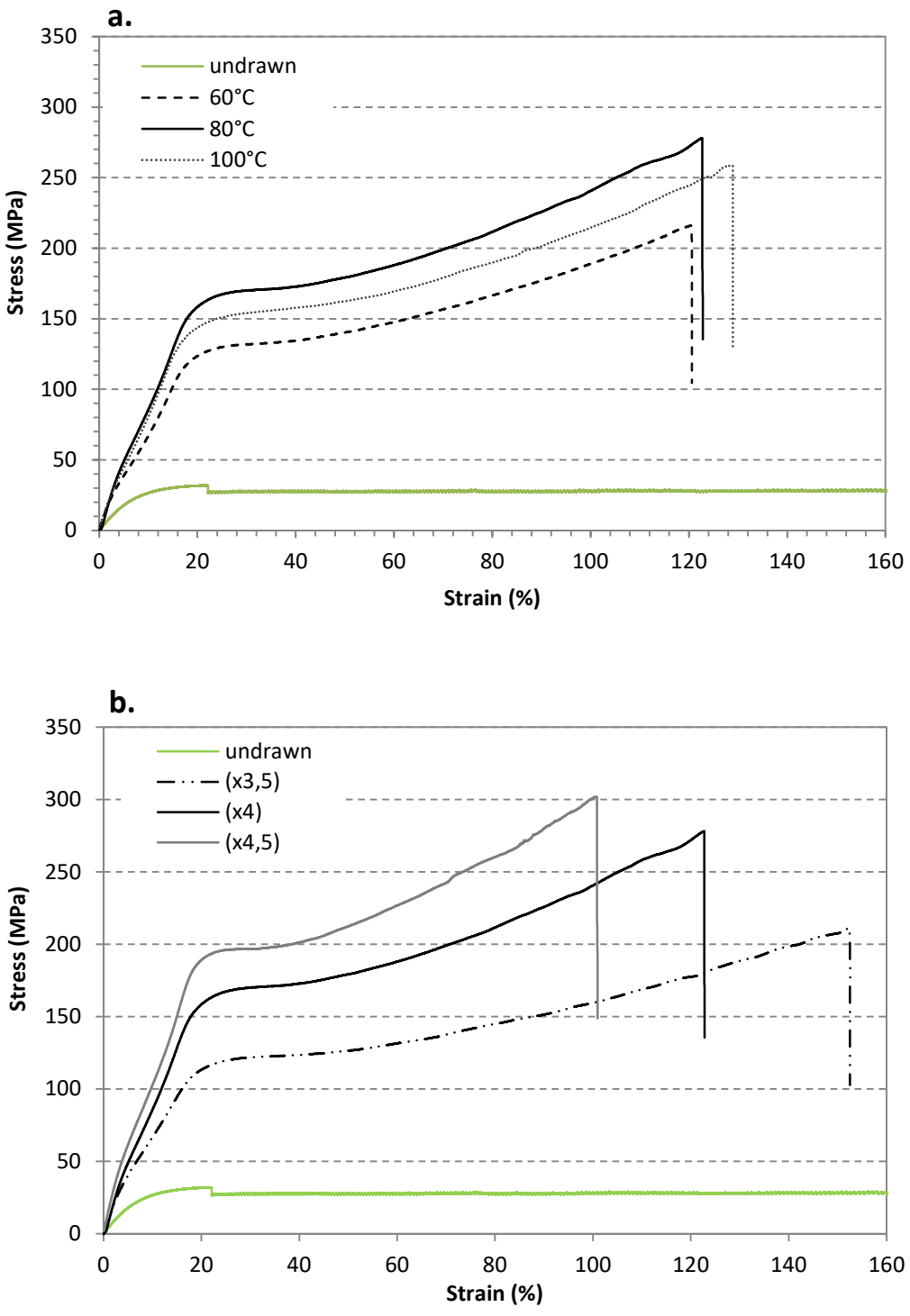

Figure 1: Evolution of the tensile behavior of the PBS monofilament drawn at different temperatures for a constant draw ratio of 4 (a) and at a different draw ratio for a constant temperature of 80°C (b). The undrawn behavior of the PBS monofilament is shown in green.

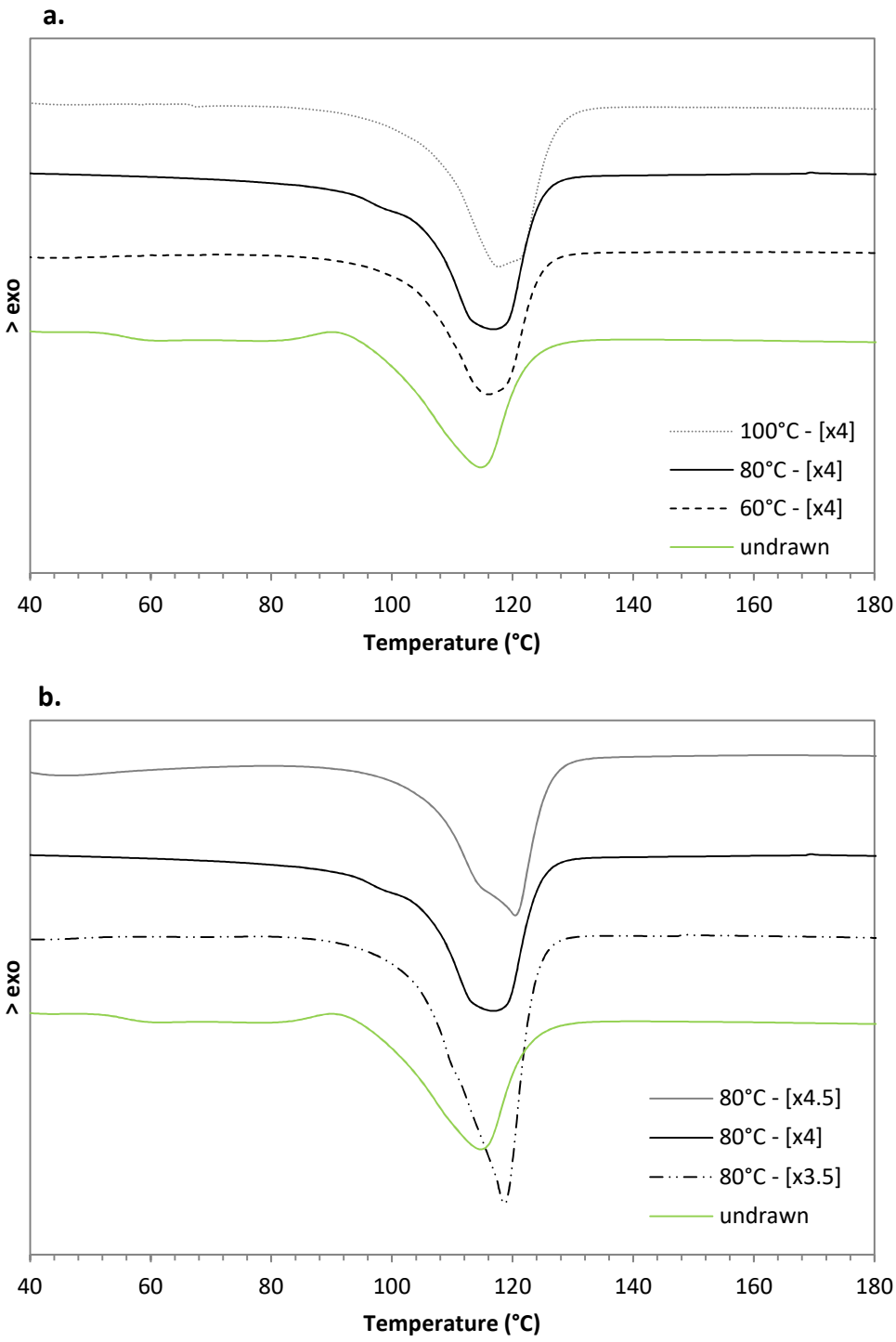

Figure 2: Evolution of the melting enthalpy behavior of the PBS monofilament drawn at different temperatures (a) and at different draw ratios (b). The undrawn behavior of the PBS monofilament is shown in green.

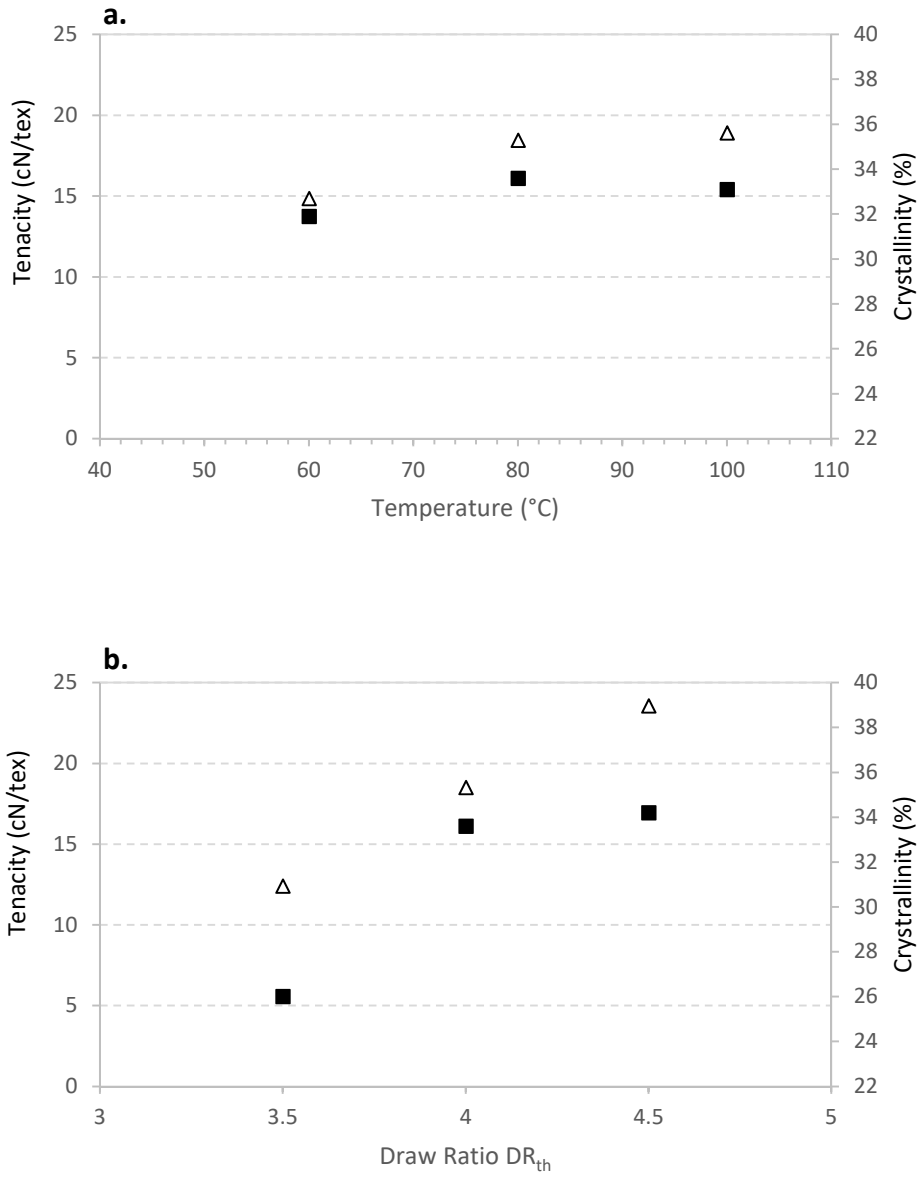

Figure 3: Relation between the evolution of tenacity (Δ) and crystallinity (■) as a function of different parameters for the draw ratio and temperature.

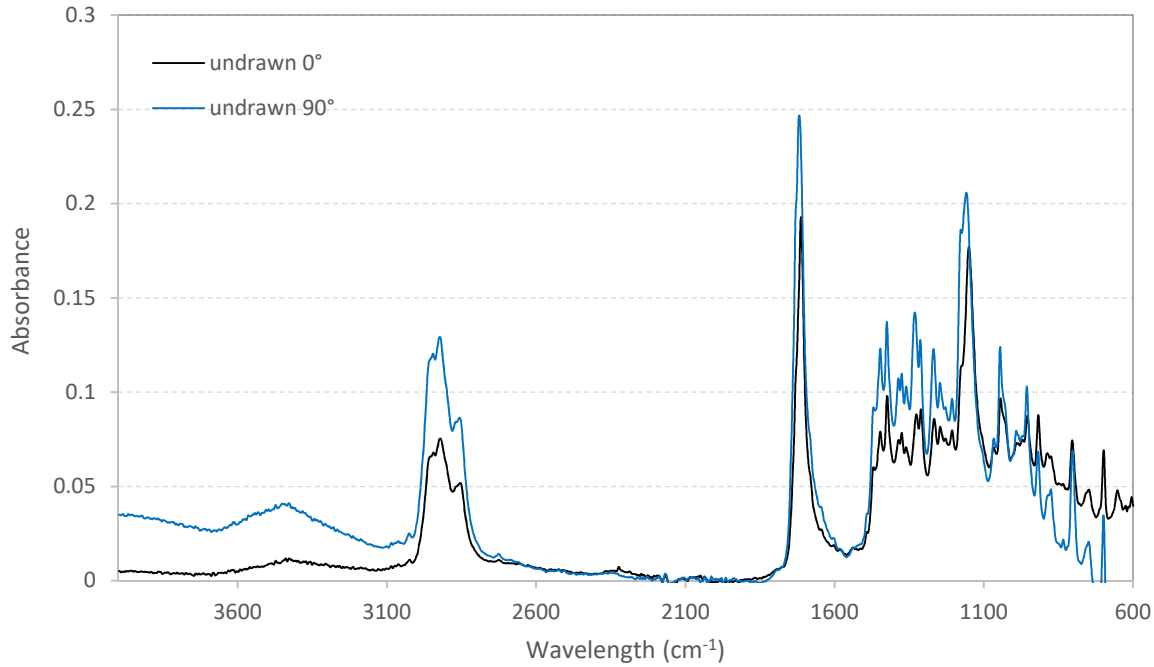

Figure 4: Polarized emission of spectrum at 0° and 90° of the PBS undrawn monofilament.

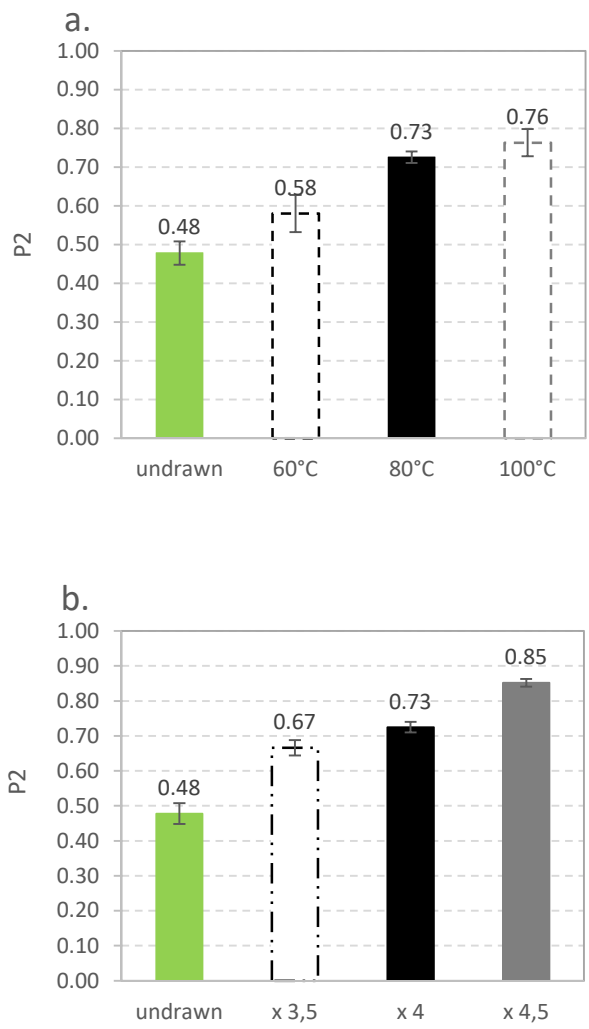

Figure 5: Evolution of the orientation function P2 for the undrawn and drawn PBS monofilament, at different drawing temperatures (a) and at different draw ratios (b).

Table 1: Mechanical properties of PBS before and after drawing in different conditions and evolution of properties.

	Draw Ratio	Temp (°C)	E (MPa)	*Gain (%)*	σ_b (MPa)	*Gain (%)*	ε (%)	*Gain (%)*	F (N)	Tenacity (cN/tex)	*Gain (%)*
Undrawn	-	-	564 ± 43		64 ± 0.5		503 ± 81.2		66 ± 1	4.2	
Drawn	x4	**60**	1014 ± 66	*+79 %*	214 ± 9.9	*+234 %*	113.3 ± 9.9	*-78 %*	244 ± 15	14.9	*+254 %*
	x4	**80**	1312 ± 44	*+132 %*	267 ± 13	*+317 %*	122.7 ± 4.3	*-76 %*	255 ± 6	18.5	*+340 %*
	x4	**100**	1037 ± 43	*+83 %*	243 ± 17	*+279 %*	127.3 ± 6.8	*-75 %*	266 ± 11	18.9	*+350 %*
	x3.5	80	1076 ± 30	*+91 %*	209 ± 11	*+226 %*	148 ± 6.8	*-71 %*	262 ± 10	12.4	*+195 %*
	x4	80	1312 ± 44	*+132 %*	267 ± 13	*+317 %*	122.7 ± 4.3	*-76 %*	255 ± 6	18.5	*+340 %*
	x4.5	80	1483 ± 184	*+162 %*	302 ± 08	*+371 %*	107.6 ± 8.8	*-79 %*	247 ± 11	23.6	*+461 %*

Table 2: Evolution of thermal transition of PBS samples before and after drawing in different conditions

	Draw ratio	Temp (°C)	Tm_1 (°C)	ΔHm_1 (J/g)	Tc (°C)	ΔHc (J/g)	Tm_{2nd} (°C)	ΔHm_2 (J/g)	χ_1 (%)
Undrawn	-	-	115.8	33.2	77.0	36.5	111.4	36.4	16.6
Drawn	x 4	**60**	118.0	63.8	77.3	54.9	113.3	49.1	31.9
	x 4	**80**	117.3	67.1	77.7	57.3	113.7	51.5	33.6
	x 4	**100**	117.3	66.3	78.0	52.2	111.7	50.1	33.1
	x **3.5**	80	117.0	51.9	77.3	44.6	113.7	39.0	26.0
	x **4**	80	117.3	67.1	77.7	57.3	113.7	49.0	33.6
	x **4.5**	80	118.7	68.5	77.7	56.7	114.3	50.0	34.2

$_{1,2}$ corresponding to first and second heating respectively

Table 3: Representation of the absorbance obtained after polarized spectra in a parallel or perpendicular direction for the peak at 2850 cm^{-1} and determination of the dichroic ratio R and the orientation function P2.

	Draw Ratio	Temp (°C)	$A_{0°}$	$A_{90°}$	R	P2*
undrawn	-	-	0.043	0.072	0.60	0.48
drawn	x 4	**60**	0.021	0.04	0.53	0.58
	x 4	**80**	0.021	0.049	0.43	0.73
	x 4	**100**	0.017	0.042	0.40	0.76
	x **3.5**	80	0.021	0.045	0.47	0.67
	x **4**	80	0.021	0.049	0.43	0.73
	x **4.5**	80	0.014	0.04	0.35	0.85

** calculated according to the equation 4*